Published in final edited form as:
*Virology*. 2008 November 25; 381(2): 194–202. doi:10.1016/j.virol.2008.08.027.

# Tyrosine phosphorylation of AAV2 vectors and its consequences on viral intracellular trafficking and transgene expression

**Li Zhong**[a,b,c,d], **Baozheng Li**[a], **Giridhararao Jayandharan**[a], **Cathryn S. Mah**[a,b,c,d], **Lakshmanan Govindasamy**[e,b,c], **Mavis Agbandje-McKenna**[e,b,c], **Roland W. Herzog**[a,b,c,f], **Kirsten A. Weigel-Van Aken**[a,b,c,d,f], **Jacqueline A. Hobbs**[c,f,g], **Sergei Zolotukhin**[a,b,c,d,f], **Nicholas Muzyczka**[b,c,d,f], and **Arun Srivastava**[a,b,c,d,f,*]

a*Division of Cellular and Molecular Therapy, Department of Pediatrics, University of Florida, College of Medicine, Gainesville, FL, USA*

b*Powell Gene Therapy Center, University of Florida, College of Medicine, Gainesville, FL, USA*

c*Genetics Institute, University of Florida, College of Medicine, Gainesville, FL, USA*

d*Shands Cancer Center, University of Florida, College of Medicine, Gainesville, FL, USA*

e*Department of Biochemistry & Molecular Biology, University of Florida, College of Medicine, Gainesville, FL, USA*

f*Department of Molecular Genetics & Microbiology, University of Florida, College of Medicine, Gainesville, FL, USA*

g*Department of Psychiatry, University of Florida, College of Medicine, Gainesville, FL, USA*

## Abstract

We have documented that epidermal growth factor receptor protein tyrosine kinase (EGFR-PTK) signaling negatively affects intracellular trafficking and transduction efficiency of recombinant adeno-associated virus 2 (AAV2) vectors. Specifically, inhibition of EGFR-PTK signaling leads to decreased ubiquitination of AAV2 capsid proteins, which in turn, facilitates viral nuclear transport by limiting proteasome-mediated degradation of AAV2 vectors. In the present studies, we observed that AAV capsids can indeed be phosphorylated at tyrosine residues by EGFR-PTK in *in vitro* phosphorylation assays and that phosphorylated AAV capsids retain their structural integrity. However, although phosphorylated AAV vectors enter cells as efficiently as their unphosphorylated counterparts, their transduction efficiency is significantly reduced. This reduction is not due to impaired viral second-strand DNA synthesis since transduction efficiency of both single-stranded AAV (ssAAV) and self-complementary AAV (scAAV) vectors is decreased by ~68% and ~74%, respectively. We also observed that intracellular trafficking of tyrosine-phosphorylated AAV vectors from cytoplasm to nucleus is significantly decreased, which leads to ubiquitination of AAV capsids followed by proteasome-mediated degradation, although downstream consequences of capsid ubiquitination may also be affected by tyrosine-phosphorylation. These studies provide new insights into the role of tyrosine-phosphorylation of AAV capsids in various steps in the virus life cycle, which has implications in the optimal use of recombinant AAV vectors in human gene therapy.

*Corresponding author: Dr. Arun Srivastava, Division of Cellular and Molecular Therapy, Cancer and Genetics Research Complex, 1376 Mowry Road, Room 492-A University of Florida College of Medicine, Gainesville, FL 32610, USA, Tel: 1-352-273-8259, Fax: 1-352-273-8342, *E-mail address*: aruns@peds.ufl.edu.

**Keywords**

AAV2 Vectors; Capsid Proteins; Tyrosine-Phosphorylation; Ubiquitination; Proteasomes; Intracellular Trafficking; Gene Expression; Gene Therapy

## Introduction

Recombinant adeno-associated virus 2 (AAV2) vectors have gained attention as an alternative to the more commonly used retrovirus- and adenovirus-based vectors for gene transfer and gene therapy (Berns and Giraud, 1996; Muzyczka, 1992). A number of Phase I/II clinical trials have been initiated, or are currently underway, that utilize recombinant AAV2 vectors for the potential gene therapy of human diseases such as cystic fibrosis, α-1 anti-trypsin deficiency, Parkinson's disease, Batten's disease, and muscular dystrophy (Flotte et al., 1996; Flotte et al., 2004; Kay et al., 2000; Snyder and Francis, 2005). Recombinant AAV2 vectors have also been reported to transduce a wide variety of cells and tissues *in vitro* and *in vivo* (Flotte et al., 1993; Muzyczka, 1992; Snyder et al., 1997; Xiao, Li, and Samulski, 1996). Several fundamental steps in the life cycle of AAV2 vectors, such as viral binding and entry (Kashiwakura et al., 2005; Qing et al., 1999; Summerford, Bartlett, and Samulski, 1999; Summerford and Samulski, 1998), intracellular trafficking (Douar et al., 2001; Hansen et al., 2000; Hansen, Qing, and Srivastava, 2001; Sanlioglu et al., 2000; Zhao et al., 2006), uncoating (Thomas et al., 2004; Zhong et al., 2004c), second-strand DNA synthesis and transgene expression (Ferrari et al., 1996; Fisher et al., 1996; Qing et al., 1997; Zhong et al., 2004a; Zhong et al., 2004b; Zhong et al., 2004d; Zhong et al., 2008b), and viral genome integration into host cell chromosome (McCarty, Young, and Samulski, 2004; Tan et al., 2001; Zhong et al., 2006), have been studied extensively.

Previous studies have shown that the ubiquitin–proteasome pathway plays a critical role in intracellular trafficking of AAV2 vectors (Ding et al., 2005; Ding et al., 2006; Douar et al., 2001; Duan et al., 2000). We recently reported that perturbations in EGFR-PTK signaling affects AAV2 transduction efficiency by not only augmenting viral second-strand DNA synthesis, but also by facilitating intracellular trafficking from the cytoplasm to nucleus (Zhong et al., 2007). These studies led to the hypothesis that prior to exiting the late endosomes, intact AAV2 particles become phosphorylated at tyrosine residues by EGFR-PTK, which leads to ubiquitination and subsequent degradation of a substantial fraction of the vectors by the cytoplasmic proteasomes, which negatively impacts the efficiency of their transport to the nucleus.

We report here that intact AAV2 capsids can be phosphorylated at tyrosine residues by EGFR-PTK, but not at serine/threonine residues by casein kinase II (CKII), under cell-free conditions *in vitro*. We also document that tyrosine-phosphorylation of AAV2 capsids negatively affects the viral intracellular trafficking and transgene expression in intact cells *in vivo*. These studies provide new insights into the role of tyrosine-phosphorylation of AAV2 capsid in various steps in the life cycle of AAV2, which have implications in the optimal use of recombinant AAV2 vectors in human gene therapy.

## Results

### Intact AAV2 capsids can be phosphorylated at tyrosine residues by EGFR-PTK, but not at serine/threonine residues by CKII, in in vitro phosphorylation assays

One of the predictions from our recently published model was that AAV2 vectors become phosphorylated at tyrosine residues by EGFR-PTK in the late endosome (Zhong et al., 2007). However, whether intact AAV2 capsid proteins can be phosphorylated at tyrosine and/or

serine/threonine residues has not been reported. Using *in vitro* phosphorylation assays, we first examined whether intact or denatured AAV2 capsid could be phosphorylated by casein kinase II (CKII) or EGFR-PTK. As shown in Fig. 1, the results clearly indicate that denatured AAV2 capsid proteins (lanes 5 and 8) can be readily phosphorylated *in vitro* by CKII and EGFR-PTK at serine/threonine and tyrosine residues, respectively. However, intact AAV2 capsids could not be phosphorylated by CKII (lane 4), but phosphorylation at tyrosine residues by EGFR-PTK was readily observed (lane 7). Tyrosine-phosphorylation of AAV2 capsids by EGFR-PTK occurred regardless of the vector production method or the encapsidated transgene. For example, Western blot analyses using anti-phospho-tyrosine (anti-p-Tyr) antibody revealed that phospho-tyrosines could not be detected in single-stranded AAV2 (ssAAV2) vectors containing the canine adiponectin gene (K9) produced by the baculovirus-based packaging system, or ssAAV2 vectors containing the red florescence protein (RFP), or self-complementary AAV2 (scAAV2) vectors containing the enhanced green fluorescent protein (EGFP) gene generated by the 293 cell-based packaging system (Fig 2A, lanes 3, 5, 7). However, all vector preparations could be phosphorylated by EGFR-PTK (Fig 2A, lanes 4, 6, 8). We also examined whether *in vitro* phosphorylation conditions *per se* lead to vector instability. To this end, following *in vitro* phosphorylation of AAV2 capsids by EGFR-PTK, intact virions (> 100 kDa) were separated from free capsid proteins (30–100 kDa) using centrifugal filter devices [(Ultracel YM-100 (KD) and YM-30 (KD)] and analyzed on Western blots using anti-p-Tyr antibody for detection of phospho-tyrosine containing capsid proteins as well as anti-AAV2 capsid (B1) antibody for detection of total capsid proteins. As shown in Fig. 2B, both the tyrosine phosphorylated (Upper Panel) and AAV2 capsid proteins (Lower Panel) were detected in the >100 kDa fraction (lanes 5, 6). No signals were detected in the 30–100 kDa fraction (lanes 8, 9). We conclude, therefore, that tyrosine- phosphorylated AAV2 vectors retain their structural integrity.

## Tyrosine phosphorylated AAV2 vectors are infectious, but their transduction efficiency is significantly reduced

We next evaluated whether tyrosine-phosphorylation affected the biological activity of AAV2 vectors by examining their ability to bind and enter the target cell as well as their ability to express the encapsidated transgene. For the first set of experiments, recombinant AAV2-*lacZ* vectors were pre-incubated with ATP alone, EGFR-TPK alone, or ATP+EGFR-PTK, and used to infect HeLa cells at 37°C for 2 hrs under identical conditions. Following exhaustive digestion with trypsin to remove any free virions, low-$M_r$ DNA samples were isolated at 2 hrs post-infection and analyzed on DNA slot-blots using a $^{32}$P-labeled *lacZ* DNA probe. As can be seen in Fig 3, *in vitro* phosphorylation of AAV2 capsids by EGFR-PTK had no effect on viral binding and entry into HeLa cells.

For the second set of experiments, both ssAAV2 and scAAV2 vectors were used since tyrosine-phosphorylation negatively affects viral second-strand DNA synthesis of ssAAV2 vectors (Mah et al., 1998; Qing et al., 2001; Qing et al., 1997; Zhong et al., 2004a; Zhong et al., 2004b; Zhong et al., 2004d), and scAAV2 vectors bypass the requirement for viral second-strand DNA synthesis (McCarty et al., 2003; Wang et al., 2003). HeLa cells were mock-infected or infected with ssAAV2-RFP or scAAV2-EGFP vectors, which were either mock-treated or incubated with ATP alone, EGFR-PTK alone, or ATP+EGFR-PTK, as described above. Transgene expression was detected by fluorescence microscopy 48 hrs post-infection. As is evident from the results shown in Fig 4, *in vitro* phosphorylation of viral capsids by EGFR-PTK decreased transgene expression by ~68% for ssAAV2 vectors (Panels A, B) and by ~74% for scAAV2 vectors (Panels C, D). Treatment of viral capsids with CKII, on the other hand, had no effect by either ssAAV2 vectors (Panels A, B) or scAAV2 vectors (Panels C, D). Thus, we conclude that although tyrosine-phosphorylated AAV2 vectors enter cells as efficiently as their unphosphorylated counterparts, their transduction efficiency is significantly

reduced. This reduction is not due to impaired viral second-strand DNA synthesis since transduction efficiency of both ssAAV2 and scAAV2 vectors is affected.

### AAV2 capsids are phosphorylated at tyrosine residues following infection, and in vitro phosphorylation of viral capsids at tyrosine residues leads to ubiquitination of intact AAV2 vectors

Since AAV2 vectors could be phosphorylated by EGFR-PTK *in vitro*, we also wished to evaluate whether intact AAV2 particles also undergo tyrosine-phosphorylation following infection. This was carried out as follows. HeLa cells were either mock-treated or treated with sodium orthovanadate (NaOV), a specific inhibitor of protein phosphatases, and then were either mock-infected or infected with AAV2 vectors for 2 hrs at 37°C. Whole cell lysates (WCLs) were prepared 4 hrs post-infection and equivalent amounts of proteins were immuno-precipitated first with anti-AAV2 capsid antibody (A20) followed by Western blot analyses using anti-p-Tyr antibody. These results are shown in Fig. 5A. As can be seen, tyrosine-phosphorylated AAV2 capsid proteins (P-Tyr-AAV2 Cap) were readily detectable in AAV2-infected cells (lanes 1, 2). No signal was detectable in mock-infected cells (lane 3), and the extent of tyrosine phosphorylation of AAV2 capsid proteins was increased following treatment with NaOV (lane 2). These results suggest that AAV2 vectors are indeed phosphorylated at tyrosine residues following infection of cells.

We next examined why tyrosine-phosphorylated AAV2 vectors failed to efficiently transduce the target cell. The ubiquitin-proteasome pathway plays an important role in the cell by specifically degrading both endogenous and foreign proteins (Pickart, 2001; Schwartz and Ciechanover, 1999). Direct evidence for ubiquitination of AAV2 capsid proteins in HeLa cells and in *in vitro* ubiquitination assays has been reported (Yan et al., 2002), where only denatured AAV2 capsids, but not intact AAV2, could be ubiquitinated *in vitro*, which suggested that either a conformational change or a modification, such as phosphorylation of intact AAV2 capsid is required before ubiquitination can ensue. A number of studies have reported that phosphorylation of cellular proteins at tyrosine or serine/threonine residues is required for efficient ubiquitination and degradation of these proteins (Brown et al., 1995; Cenciarelli et al., 1996; Paolini et al., 1999; Penrose et al., 2004).

Since in our previously published studies (Zhong et al., 2007), we reported that inhibition of EGFR-PTK signaling decreases ubiquitination of total cellular proteins as well as AAV2 capsid proteins, we examined whether *in vitro* phosphorylation of viral capsids by EGFR-PTK leads to ubiquitination of AAV2 capsids in intact cells. This was carried out as follows. HeLa cells were either mock-treated or treated with MG132, a specific inhibitor of proteasomes, and then were either mock-infected or infected with AAV2 vectors, with and without tyrosine-phosphorylation, for 2 hrs at 37°C. Whole cell lysates (WCLs) were prepared 4 hrs post-infection and equivalent amounts of proteins were immuno-precipitated first with anti-AAV2 capsid antibody (A20) followed by Western blot analyses using anti-Ub monoclonal antibody. These results are shown in Fig. 5B. As can be seen, the ubiquitinated AAV2 capsid proteins (Ub-AAV2 Cap) were undetectable in mock-infected cells (lanes 1, 2), the signal of ubiquitinated AAV2 capsid proteins was weaker in untreated cells (lanes 3, 5, 7, 9), but a significant accumulation of ubiquitinated AAV2 capsid proteins occurred following treatment with MG132 (lanes 4, 6, 8, 10). Most interestingly, *in vitro* phosphorylation of viral capsids by EGFR-PTK dramatically increased the extent of accumulation of MG132-induced ubiquitinated AAV2 capsid proteins (lane 6). These results strongly suggest that *in vitro* phosphorylation of capsids by EGFR-PTK leads to ubiquitination of AAV2 capsids in intact cells. The authors might want to discuss alternative interpretations of the results. However, since MG132 potentiates capsid ubiquitination as well as increases transduction, it is also possible that capsid ubiquitination serves as a positive sorting signal and not as a negative

degradation signal. Thus, tyrosine-phosphorylation of AAV2 capsids may limit transduction by affecting other events during infection.

### In vitro phosphorylation of viral capsids at tyrosine residues leads to impaired intracellular trafficking to the nucleus

The ubiquitin–proteasome pathway plays a critical role in AAV2 intracellular trafficking, and proteasome inhibitors can promote AAV2 nuclear transport, leading to augmentation of AAV2 transduction (Ding et al., 2005; Ding et al., 2006; Douar et al., 2001; Duan et al., 2000). We have also documented that inhibition of EGFR-PTK signaling facilitates nuclear transport of AAV2 vectors (Zhong et al., 2004c; Zhong et al., 2007), which suggested that phosphorylation of AAV2 capsids by EGFR-PTK might also be involved in AAV2 trafficking. To further examine this hypothesis, we examined the cytoplasmic and nuclear distribution of AAV2 genomes following *in vitro* phosphorylation of AAV2 vectors. HeLa cells were infected with AAV2-*lacZ* vectors, with or without tyrosine-phosphorylation, as described above. Nuclear and cytoplasmic fractions were obtained 18 hrs post-infection, and low-$M_r$ DNA samples were isolated and analyzed on Southern blots using a $^{32}$P-labeled *lacZ* DNA probe. These results are shown in Fig. 6, Panel A. A significant fraction of the input ssAAV2 DNA was present in the cytoplasm following infection with AAV2 vectors that were mock-treated or pre-incubated with ATP alone, or with EGFR-TPK alone (lanes 2, 3, and 4), and only a small fraction was detected in the nucleus (lanes 7, 8, 9). Interestingly, however, in cells infected with AAV2 vectors that were phosphorylated by EGFR-PTK, the input ssAAV2 DNA in the cytoplasmic fraction was increased (lane 5) with a corresponding decrease in the nuclear fraction (lane 10). Densitometric scanning of autoradiographs (Fig. 6, Panel B) indicated that ~35% of the input ssAAV2 DNA was present in the nuclear fraction in cells infected with AAV2 vectors in the absence of tyrosine-phosphorylation, but only ~16% following *in vitro* phosphorylation at tyrosine residues. These data are consistent with our previous studies (Zhong et al., 2007), and corroborate that intracellular trafficking of tyrosine- phosphorylated AAV2 vectors from the cytoplasm to the nucleus is significantly decreased, which is due most likely to increased ubiquitination of AAV2 capsids followed by proteasome-mediated degradation.

## Discussion

Our original observation that specific inhibitors of cellular protein tyrosine kinases in general, and EGFR-PTK in particular, but not inhibitors of cellular serine/threonine kinases, dramatically increase the transduction efficiency of ssAAV vectors (Mah et al., 1998; Qing et al., 1997), prompted us to pursue a series of studies in which we identified that a cellular chaperone protein, FKBP52, is phosphorylated at tyrosine residues by EGFR-PTK, and that tyrosine-phosphorylated FKBP52 strongly inhibits the viral second-strand DNA synthesis, and consequently the transgene expression (Qing et al., 2001; Qing et al., 2003; Zhong et al., 2004a; Zhong et al., 2004b; Zhong et al., 2004d; Zhong et al., 2008b). More recently, however, we observed that in addition to negatively impacting viral second-strand DNA synthesis and transgene expression in the nucleus, EGFR-PTK-signaling also negatively regulates viral intracellular trafficking in the cytoplasm (Zhong et al., 2007). Based on these studies, we hypothesized that either prior to or during viral egress from the late endosome, EGFR-PTK catalyzes the phosphorylation of intact AAV2 capsids, which is a putative signal for ubiquitination. Ubiquitinated AAV2 capsids are subsequently targeted for degradation by the cellular proteasome. That intact AAV2 vectors can indeed be phosphorylated at tyrosine residues by EGFR-PTK, both *in vitro* and *in vivo*, but not at serine/threonine residues by CKII, as described in the present studies, lends strong support to our hypothesis.

Although the Ub/proteasome pathway has previously been shown to play an essential role in AAV2 nuclear transport (Ding et al., 2005; Ding et al., 2006; Douar et al., 2001; Duan et al.,

2000), our data also provide direct evidence that EGFR-PTK- mediated tyrosine phosphorylation of AAV2 capsids leads to ubiquitination, and subsequent degradation by the proteasome, which impairs viral nuclear transport as well as transduction efficiency of AAV2 vectors. Whether AAV2 vectors can be phosphorylated at serine/threonine residues by other cellular serine/threonine kinase(s), and what consequences, if any, of serine/threonine phosphorylation of capsids have on the wild-type (WT) AAV2 biology, remains unclear. What has become clear from our current studies is that phosphorylation of the surface-exposed tyrosine residues on recombinant AAV2 vector capsids is not desirable since site-directed mutagenesis of these tyrosine residues resulted in the generation of AAV2 vectors that are capable of transducing a wide variety of cells and tissues *in vitro* and *in vivo* significantly more efficiently than those with the WT capsids (Zhong et al., 2008a).

Further studies on the precise role of tyrosine-phosphorylation of AAV2 capsids are likely to lead not only to a better understanding of various steps in the virus life cycle, but also to aid in the development of novel recombinant AAV vectors especially in view of the fact that the surface-exposed tyrosine residues are conserved in AAV serotypes 1 through 10, which has implications in the potential use of AAV serotype vectors in human gene therapy.

## Materials and Methods

### Cells, viruses, plasmids, antibodies, and chemicals

The human cervical carcinoma cell line, HeLa, was obtained from the American Type Culture Collection (ATCC, Rockville, MD). The cell line was maintained as monolayer cultures in Iscove's-modified Dulbecco's medium (IMDM) supplemented with 10% newborn calf serum (NCS) and 1% (by volume) of 100× stock solution of antibiotics (10,000 U penicillin+10,000 μg streptomycin). Highly purified stocks of ssAAV2 vectors containing the β-galactosidase (*lacZ*) reporter gene, red fluorescence protein (RFP) gene, or scAAV2 vectors containing the enhanced green fluorescence protein (EGFP) gene driven by the chick β-actin (CBA) promoter (ssAAV2-*lacZ*, ssAAV2-RFP, or scAAV2-EGFP) were generated as described previously (Auricchio et al., 2001). ssAAV2 vectors containing the canine adiponectin gene (ssAAV2-K9) were generated by a baculovirus-based packaging system as described previously (Urabe, Ding, and Kotin, 2002). Physical particle titers of recombinant vector stocks were determined by quantitative DNA slot blot analysis. An AAV2-helper plasmid, pACG-2, containing the AAV2 *rep* gene with an ACG start codon, was generously provided by Dr. R. Jude Samulski (University of North Carolina at Chapel Hill, Chapel Hill, NC). A self-complementary AAV2 (scAAV2) cloning vector, pdsCBA-EGFP, was a kind gift from Dr. Xiao Xiao (University of North Carolina at Chapel Hill). Horseradish peroxidase (HRP)–conjugated antibody specific for ubiquitin (Ub) (mouse monoclonal immunoglobulin $G_1$ [$IgG_1$], clone P4D1), antibody specific for phosphorylated tyrosine residues (anti-p-Tyr) (mouse monoclonal $IgG_{2b}$, clone PY99), HRP-conjugated goat anti-mouse $IgG_{2b}$ antibody, HRP-conjugated goat anti-mouse $IgG_1$ antibody, normal mouse IgG and protein G plus-agarose were purchased from Santa Cruz Biotechnology (Santa Cruz, CA). Antibody specific for intact AAV2 particles (mouse monoclonal $IgG_3$, clone A20) and antibody specific for AAV2 capsid proteins (mouse monoclonal IgG1, clone B1) were obtained from Research Diagnostics, Inc. (Flanders, NJ). MG132 was purchased from Calbiochem (La Jolla, CA). All other chemicals were purchased from Sigma-Aldrich Co. (St. Louis, MO).

### In vitro phosphorylation assays

*In vitro* phosphorylation by CKII (Calbiochem, La Jolla, CA) was carried out as previously described (Qing et al., 2001; Zhong et al., 2004d). Briefly, the complete reaction mixture contained identical amount of intact or denatured AAV2 vectors (~$3–4.8\times10^{10}$ viral particles), 20 mM Tris-HCl, 50 mM KCl, 10 mM $MgCl_2$, 50 mM $Na_3VO4$, 10 μCi (0.37 mBq) γ-$^{32}$P-

ATP and 500 U (500,000 U/ml) purified CKII. *In vitro* phosphorylation by EGFR-PTK was carried out as described previously (Qing et al., 2001; Weber, Bertics, and Gill, 1984; Zhong et al., 2004d), with the following modifications. The complete reaction mixture contained identical amounts of intact or denatured AAV2 vectors (~3–4.8×$10^{10}$ viral particles), 20 mM HEPES, 4 mM $MgCl_2$, 10 mM $MnCl_2$, 10 μCi (0.37 mBq) γ-$^{32}$P-ATP and 10 U (15,000 U/mg) purified EGFR-PTK (Sigma-Aldrich Co., St. Louis, MO) with the indicated appropriate controls. The reaction mixtures were incubated at 30°C for 1 hr. The phosphorylated AAV2 capsid proteins were separated from free γ-$^{32}$P-ATP on 10% SDS-polyacrylamide gels followed by autoradiography with Kodak 7 X-Omat film at −70°C. In some experiments, *in vitro* phosphorylation assays by EGFR-PTK were also carried out by adding 200 μM ATP instead of γ-$^{32}$P-ATP. The phosphorylated AAV2 capsid proteins were identified by Western blotting with anti-p-Tyr antibody as described below.

### Separation of intact AAV2 virions and AAV2 capsid proteins using ultrafiltration assay

After *in vitro* phosphorylation assays, the reaction samples plus 450 μL of phosphate buffered saline (PBS, pH7.4) were added into the upper part of the YM-100 Microcon® centrifugal filter device (cutoff value: 100 kDa) (Millipore Corporation, Bedford, MA) and centrifuged at 14,000×g for 24 min at 4°C. Approximately 10–20 μL of ultrafiltrates were collected. The flow through samples were added into the upper part of the YM-30 Microcon® centrifugal filter device (cutoff value: 30 kDa) (Millipore Corporation, Bedford, MA) and centrifuged at 14,000×g for 24 min at 4°C. Approximately 10–20 μL of ultrafiltrates were collected. The ultrafiltrate samples were analyzed by Western blotting using anti-p-Tyr and anti-AAV2 cap (B1) antibodies as described below.

### Preparation of whole cell lysates (WCLs) and co-immunoprecipitations

WCLs were prepared as described previously (Zhao et al., 2006; Zhong et al., 2004d; Zhong and Su, 2002), with the following modifications. Briefly, 2×$10^6$ HeLa cells were either mock-treated, treated with, 1 mM NaOV for 2 hrs and then were infected with AAV2-adiponectin vectors at $10^4$ particles/cell for 2 hrs at 37°C. In some experiments cells were either mock-treated or treated with 4 μM MG132 for 4 hrs and then were infected with AAV2-adiponectin vectors at $10^4$ particles/cell for 2 hrs at 37°C, which were mock-incubated or pre-incubated with ATP, EGFR-TPK, or both. For immunoprecipitations, cells were treated with 0.01% trypsin and washed extensively with PBS to remove any adsorbed and unadsorbed virus particles after treatment or at 4 hrs post-infection and then resuspended in 1 ml hypotonic buffer (20 mM HEPES pH 7.5, 5 mM KCl, 0.5 mM $MgCl_2$) containing 1 mM DTT, 10 mM NaF, 2 mM $Na_3VO_4$, 0.5 mM PMSF, 10 μg/ml aprotinin, 10 μg/ml leupeptin and 10 μg/ml. WCLs were prepared by homogenization in a tight-fitting Duall tissue grinder until about 95% cell lysis was achieved as monitored by trypan blue dye exclusion assay. WCLs were cleared of non-specific binding by incubation with 0.25 mg of normal mouse IgG together with 20 μl of protein G plus-agarose beads for 60 min at 4°C in an orbital shaker. After preclearing, 2 μg of capsid antibody against intact AAV2 particles (A20) (mouse $IgG_3$) or 2 μg of normal mouse IgG (as a negative control) was added and incubated at 4°C for 1 hr, followed by precipitation with protein G-agarose beads at 4°C for 12 hrs in a shaker. Pellets were collected by centrifugation at 2,500 rpm for 5 min at 4°C and washed four times with PBS. After the final wash, supernatants were aspirated and discarded, and pellets were resuspended in equal volume of 2× SDS sample buffer. Twenty μl of resuspended pellet solutions were used for Western blotting with HRP–conjugated anti-Ub antibody as described below.

### Western blot analyses

Western blotting was performed as described previously (Zhao et al., 2006; Zhong et al., 2004d; Zhong and Su, 2002). For *in vitro* phosphorylation assays, the reaction mixtures were

separated by 10% SDS- polyacrylamide gel electrophoresis (SDS-PAGE) and transferred to Immobilon-P membranes (Millipore, Bedford, MA). Membranes were blocked at 4°C for 12 hrs with 5% nonfat milk in 1×Tris-buffered saline (TBS, 20 mM Tris-HCl, pH 7.5, 150 mM NaCl). Membranes were treated with monoclonal anti-p-Tyr antibody (1:300 dilution) or monoclonal anti-AAV2 capsid proteins antibody followed by horseradish peroxidase–conjugated anti-mouse $IgG_{2b}$ or anti-mouse $IgG_1$ (1:10,000 dilution). For immunoprecipitations, resuspended pellet solutions were boiled for 2–3 min and 20 μl of samples were used for SDS-PAGE. After blocking at 4°C for 12 hrs with 5% nonfat milk in 1×Tris-buffered saline, membranes were treated with monoclonal HRP-conjugated anti-Ub antibody (1:2,000 dilution). Immuno- reactive bands were visualized using chemiluminescence (ECL–plus, Amersham Pharmacia Biotech, Piscataway, NJ).

### Isolation of nuclear and cytoplasmic fractions from HeLa cells

Nuclear and cytoplasmic fractions from HeLa cells were isolated as described previously (Zhong et al., 2004c; Zhong et al., 2007). Briefly, mock-infected or recombinant ssAAV2-*lacZ* vector-infected cells were washed twice with PBS at 18 hrs post-infection, treated with 0.01% trypsin and washed extensively with PBS to remove any adsorbed and unadsorbed virus particles. Cell pellets were gently resuspended in 200 μl hypotonic buffer (10 mM HEPES, pH 7.9, 1.5 mM $MgCl_2$, 10 mM KCl, 0.5 mM DTT, 0.5 mM PMSF) and incubated on ice for 5 min, after which 10 μl 10% NP-40 was added, and observed under a light microscope. Samples were mixed gently and centrifuged for 5 min at 500 rpm at 4°C. Supernatants (cytoplasmic fraction) were decanted and stored on ice. Pellets (nuclear fractions) were washed twice with 1 ml hypotonic buffer and stored on ice. The purity of each fraction was determined to be > 95%, as measured by the absence of acid phosphatase activity (nuclear fractions) and absence of histone H3 (cytoplasmic fractions) as described previously (Hansen et al., 2000; Zhong et al., 2004c).

### Southern blot analysis for AAV2 trafficking

Low-$M_r$ DNA samples from nuclear and cytoplasmic fractions were isolated and electrophoresed on 1% agarose gels or 1% alkaline-agarose gels followed by Southern blot hybridization using a $^{32}$P-labeled *lacZ*-specific DNA probe as described previously (Hansen et al., 2000; Zhong et al., 2004c). Densitometric scanning of autoradiographs for the quantitation was evaluated with ImageJ analysis software (NIH, Bethesda, MD).

### Recombinant AAV2 vector transduction assays

Approximately $1\times10^5$ HeLa cells were plated in each well in 12-well plates and incubated at 37°C for 12 hrs. Cells were washed once with IMDM and then infected at 37°C for 2 hrs with recombinant AAV2 vectors as described previously (Qing et al., 2001; Zhong et al., 2004a; Zhong et al., 2004d). Cells were incubated in complete IMDM containing 10% NCS and 1% antibiotics for 48 hrs. The transduction efficiency was measured by EGFP imaging using a Leica DM IRB/E fluorescence microscope (Leica Microsystems Wetzlar GmbH, Wetzlar, Germany). Images from three to five visual fields of mock-infected and vector- infected HeLa cells at 48 hrs post-infection were analyzed quantitatively by ImageJ analysis software (NIH, Bethesda, MD, USA). Transgene expression was assessed as total area of green fluorescence ($pixel^2$) per visual field (mean ± SD). Analysis of variance (ANOVA) was used to compare between test results and the control and they were determined to be statistically significant.

## Acknowledgments

We thank Drs. R. Jude Samulski and Xiao Xiao for their kind gifts of recombinant AAV plasmids, and Dr. Shangzhen Zhou for her help with recombinant AAV2 vectors. We also thank Drs. Kenneth I. Berns and Dennis Steindler for a critical review of this manuscript. This research was supported in part by a research grant 8187368876 from the Roche

Foundation for Anemia Research (to LZ), a Scientist Development Grant from the American Heart Association (to CSM), and Public Health Service grants R01 GM-082946 and P01 HL-51811 (to MA-M and SZ), R01 GM-082946 and P01 HL-51811 (to MA-M, NM and SZ), R01 DK-062302 (to SZ), P01 HL-078810-Project 3 (to RWH), and R01 EB-002073, R01 HL-65570 and R01 HL-07691, and P01 DK 058327-Project 1 (to AS) from the National Institutes of Health.

## References

Auricchio A, Hildinger M, O'Connor E, Gao GP, Wilson JM. Isolation of highly infectious and pure adeno-associated virus type 2 vectors with a single-step gravity-flow column. Hum Gene Ther 2001;12 (1):71–76. [PubMed: 11177544]

Berns KI, Giraud C. Biology of adeno-associated virus. Curr Top Microbiol Immunol 1996;218:1–23. [PubMed: 8794242]

Brown K, Gerstberger S, Carlson L, Franzoso G, Siebenlist U. Control of I kappa B-alpha proteolysis by site-specific, signal-induced phosphorylation. Science 1995;267(5203):1485–1488. [PubMed: 7878466]

Cenciarelli C, Wilhelm KG Jr, Guo A, Weissman AM. T cell antigen receptor ubiquitination is a consequence of receptor-mediated tyrosine kinase activation. J Biol Chem 1996;271(15):8709–8713. [PubMed: 8621503]

Ding W, Zhang L, Yan Z, Engelhardt JF. Intracellular trafficking of adeno-associated viral vectors. Gene Ther 2005;12(11):873–880. [PubMed: 15829993]

Ding W, Zhang LN, Yeaman C, Engelhardt JF. rAAV2 traffics through both the late and the recycling endosomes in a dose-dependent fashion. Mol Ther 2006;13(4):671–682. [PubMed: 16442847]

Douar AM, Poulard K, Stockholm D, Danos O. Intracellular trafficking of adeno-associated virus vectors: routing to the late endosomal compartment and proteasome degradation. J Virol 2001;75(4):1824–1833. [PubMed: 11160681]

Duan D, Yue Y, Yan Z, Yang J, Engelhardt JF. Endosomal processing limits gene transfer to polarized airway epithelia by adeno-associated virus. J Clin Invest 2000;105(11):1573–1587. [PubMed: 10841516]

Ferrari FK, Samulski T, Shenk T, Samulski RJ. Second-strand synthesis is a rate-limiting step for efficient transduction by recombinant adeno-associated virus vectors. J Virol 1996;70(5):3227–3234. [PubMed: 8627803]

Fisher KJ, Gao GP, Weitzman MD, DeMatteo R, Burda JF, Wilson JM. Transduction with recombinant adeno-associated virus for gene therapy is limited by leading-strand synthesis. J Virol 1996;70(1): 520–532. [PubMed: 8523565]

Flotte T, Carter B, Conrad C, Guggino W, Reynolds T, Rosenstein B, Taylor G, Walden S, Wetzel R. A phase I study of an adeno-associated virus-CFTR gene vector in adult CF patients with mild lung disease. Hum Gene Ther 1996;7(9):1145–1159. [PubMed: 8773517]

Flotte TR, Afione SA, Conrad C, McGrath SA, Solow R, Oka H, Zeitlin PL, Guggino WB, Carter BJ. Stable in vivo expression of the cystic fibrosis transmembrane conductance regulator with an adeno-associated virus vector. Proc Natl Acad Sci U S A 1993;90(22):10613–10617. [PubMed: 7504271]

Flotte TR, Brantly ML, Spencer LT, Byrne BJ, Spencer CT, Baker DJ, Humphries M. Phase I trial of intramuscular injection of a recombinant adeno-associated virus alpha 1-antitrypsin (rAAV2-CB-hAAT) gene vector to AAT-deficient adults. Hum Gene Ther 2004;15(1):93–128. [PubMed: 14965381]

Hansen J, Qing K, Kwon HJ, Mah C, Srivastava A. Impaired intracellular trafficking of adeno-associated virus type 2 vectors limits efficient transduction of murine fibroblasts. J Virol 2000;74(2):992–996. [PubMed: 10623762]

Hansen J, Qing K, Srivastava A. Adeno-associated virus type 2-mediated gene transfer: altered endocytic processing enhances transduction efficiency in murine fibroblasts. J Virol 2001;75(9):4080–4090. [PubMed: 11287557]

Kashiwakura Y, Tamayose K, Iwabuchi K, Hirai Y, Shimada T, Matsumoto K, Nakamura T, Watanabe M, Oshimi K, Daida H. Hepatocyte growth factor receptor is a coreceptor for adeno-associated virus type 2 infection. J Virol 2005;79(1):609–614. [PubMed: 15596854]

Kay MA, Manno CS, Ragni MV, Larson PJ, Couto LB, McClelland A, Glader B, Chew AJ, Tai SJ, Herzog RW, Arruda V, Johnson F, Scallan C, Skarsgard E, Flake AW, High KA. Evidence for gene transfer and expression of factor IX in haemophilia B patients treated with an AAV vector. Nat Genet 2000;24(3):257–261. [PubMed: 10700178]

Mah C, Qing K, Khuntirat B, Ponnazhagan S, Wang XS, Kube DM, Yoder MC, Srivastava A. Adeno-associated virus type 2-mediated gene transfer: role of epidermal growth factor receptor protein tyrosine kinase in transgene expression. J Virol 1998;72(12):9835–9843. [PubMed: 9811719]

McCarty DM, Fu H, Monahan PE, Toulson CE, Naik P, Samulski RJ. Adeno-associated virus terminal repeat (TR) mutant generates self-complementary vectors to overcome the rate-limiting step to transduction in vivo. Gene Ther 2003;10(26):2112–2118. [PubMed: 14625565]

McCarty DM, Young SM Jr, Samulski RJ. Integration of adeno-associated virus (AAV) and recombinant AAV vectors. Annu Rev Genet 2004;38:819–845. [PubMed: 15568995]

Muzyczka N. Use of adeno-associated virus as a general transduction vector for mammalian cells. Curr Top Microbiol Immunol 1992;158:97–129. [PubMed: 1316261]

Paolini R, Serra A, Molfetta R, Piccoli M, Frati L, Santoni A. Tyrosine kinase-dependent ubiquitination of CD16 zeta subunit in human NK cells following receptor engagement. Eur J Immunol 1999;29 (10):3179–3187. [PubMed: 10540329]

Penrose KJ, Garcia-Alai M, de Prat-Gay G, McBride AA. Casein Kinase II phosphorylation-induced conformational switch triggers degradation of the papillomavirus E2 protein. J Biol Chem 2004;279 (21):22430–22439. [PubMed: 15014086]

Pickart CM. Mechanisms underlying ubiquitination. Annu Rev Biochem 2001;70:503–533. [PubMed: 11395416]

Qing K, Hansen J, Weigel-Kelley KA, Tan M, Zhou S, Srivastava A. Adeno-associated virus type 2-mediated gene transfer: role of cellular FKBP52 protein in transgene expression. J Virol 2001;75 (19):8968–8976. [PubMed: 11533160]

Qing K, Li W, Zhong L, Tan M, Hansen J, Weigel-Kelley KA, Chen L, Yoder MC, Srivastava A. Adeno-associated virus type 2-mediated gene transfer: role of cellular T-cell protein tyrosine phosphatase in transgene expression in established cell lines in vitro and transgenic mice in vivo. J Virol 2003;77 (4):2741–2746. [PubMed: 12552015]

Qing K, Mah C, Hansen J, Zhou S, Dwarki V, Srivastava A. Human fibroblast growth factor receptor 1 is a co-receptor for infection by adeno-associated virus 2. Nat Med 1999;5(1):71–77. [PubMed: 9883842]

Qing K, Wang XS, Kube DM, Ponnazhagan S, Bajpai A, Srivastava A. Role of tyrosine phosphorylation of a cellular protein in adeno-associated virus 2-mediated transgene expression. Proc Natl Acad Sci U S A 1997;94(20):10879–10884. [PubMed: 9380728]

Sanlioglu S, Benson PK, Yang J, Atkinson EM, Reynolds T, Engelhardt JF. Endocytosis and nuclear trafficking of adeno-associated virus type 2 are controlled by rac1 and phosphatidylinositol-3 kinase activation. J Virol 2000;74(19):9184–9196. [PubMed: 10982365]

Schwartz AL, Ciechanover A. The ubiquitin-proteasome pathway and pathogenesis of human diseases. Annu Rev Med 1999;50:57–74. [PubMed: 10073263]

Snyder RO, Francis J. Adeno-associated viral vectors for clinical gene transfer studies. Curr Gene Ther 2005;5(3):311–321. [PubMed: 15975008]

Snyder RO, Miao CH, Patijn GA, Spratt SK, Danos O, Nagy D, Gown AM, Winther B, Meuse L, Cohen LK, Thompson AR, Kay MA. Persistent and therapeutic concentrations of human factor IX in mice after hepatic gene transfer of recombinant AAV vectors. Nat Genet 1997;16(3):270–276. [PubMed: 9207793]

Summerford C, Bartlett JS, Samulski RJ. AlphaVbeta5 integrin: a co-receptor for adeno-associated virus type 2 infection. Nat Med 1999;5(1):78–82. [PubMed: 9883843]

Summerford C, Samulski RJ. Membrane-associated heparan sulfate proteoglycan is a receptor for adeno-associated virus type 2 virions. J Virol 1998;72(2):1438–1445. [PubMed: 9445046]

Tan M, Qing K, Zhou S, Yoder MC, Srivastava A. Adeno-associated virus 2-mediated transduction and erythroid lineage-restricted long-term expression of the human beta-globin gene in hematopoietic cells from homozygous beta-thalassemic mice. Mol Ther 2001;3(6):940–946. [PubMed: 11407908]

Thomas CE, Storm TA, Huang Z, Kay MA. Rapid uncoating of vector genomes is the key to efficient liver transduction with pseudotyped adeno-associated virus vectors. J Virol 2004;78(6):3110–3122. [PubMed: 14990730]

Urabe M, Ding C, Kotin RM. Insect cells as a factory to produce adeno-associated virus type 2 vectors. Hum Gene Ther 2002;13(16):1935–1943. [PubMed: 12427305]

Wang Z, Ma HI, Li J, Sun L, Zhang J, Xiao X. Rapid and highly efficient transduction by double-stranded adeno-associated virus vectors in vitro and in vivo. Gene Ther 2003;10(26):2105–2111. [PubMed: 14625564]

Weber W, Bertics PJ, Gill GN. Immunoaffinity purification of the epidermal growth factor receptor. Stoichiometry of binding and kinetics of self-phosphorylation. J Biol Chem 1984;259(23):14631–14636. [PubMed: 6094567]

Xiao X, Li J, Samulski RJ. Efficient long-term gene transfer into muscle tissue of immunocompetent mice by adeno-associated virus vector. J Virol 1996;70(11):8098–8108. [PubMed: 8892935]

Yan Z, Zak R, Luxton GW, Ritchie TC, Bantel-Schaal U, Engelhardt JF. Ubiquitination of both adeno-associated virus type 2 and 5 capsid proteins affects the transduction efficiency of recombinant vectors. J Virol 2002;76(5):2043–2053. [PubMed: 11836382]

Zhao W, Zhong L, Wu J, Chen L, Qing K, Weigel-Kelley KA, Larsen SH, Shou W, Warrington KH Jr, Srivastava A. Role of cellular FKBP52 protein in intracellular trafficking of recombinant adeno-associated virus 2 vectors. Virology 2006;353(2):283–293. [PubMed: 16828834]

Zhong L, Chen L, Li Y, Qing K, Weigel-Kelley KA, Chan RJ, Yoder MC, Srivastava A. Self-complementary adeno-associated virus 2 (AAV)-T cell protein tyrosine phosphatase vectors as helper viruses to improve transduction efficiency of conventional single-stranded AAV vectors in vitro and in vivo. Mol Ther 2004a;10(5):950–957. [PubMed: 15509512]

Zhong L, Li B, Mah CS, Govindasamy L, Agbandje-McKenna M, Cooper MC, Herzog RW, Weigel Van-Aken KA, Hobbs JA, Zolotukhin S, Muzyczka N, Srivastava A. Next generation of recombinant adeno-associated virus 2 vectors: Point mutations in tyrosines lead to high-efficiency transduction at lower doses. Proc Natl Acad Sci U S A 2008a;105(22):7827–7832. [PubMed: 18511559]

Zhong L, Li W, Li Y, Zhao W, Wu J, Li B, Maina N, Bischof D, Qing K, Weigel Kelley KA, Zolotukhin I, Warrington KH Jr, Li X, Slayton WB, Yoder MC, Srivastava A. Evaluation of primitive murine hematopoietic stem and progenitor cell transduction in vitro and in vivo by recombinant adeno-associated virus vector serotypes 1 through 5. Hum Gene Ther 2006;17(3):321–333. [PubMed: 16544981]

Zhong L, Li W, Yang Z, Chen L, Li Y, Qing K, Weigel-Kelley KA, Yoder MC, Shou W, Srivastava A. Improved transduction of primary murine hepatocytes by recombinant adeno-associated virus 2 vectors in vivo. Gene Ther 2004b;11(14):1165–1169. [PubMed: 15164097]

Zhong L, Li W, Yang Z, Qing K, Tan M, Hansen J, Li Y, Chen L, Chan RJ, Bischof D, Maina N, Weigel-Kelley KA, Zhao W, Larsen SH, Yoder MC, Shou W, Srivastava A. Impaired nuclear transport and uncoating limit recombinant adeno-associated virus 2 vector-mediated transduction of primary murine hematopoietic cells. Hum Gene Ther 2004c;15(12):1207–1218. [PubMed: 15684697]

Zhong L, Qing K, Si Y, Chen L, Tan M, Srivastava A. Heat-shock treatment-mediated increase in transduction by recombinant adeno-associated virus 2 vectors is independent of the cellular heat-shock protein 90. J Biol Chem 2004d;279(13):12714–12723. [PubMed: 14711833]

Zhong L, Su JY. Isoflurane activates PKC and Ca(2+)-calmodulin-dependent protein kinase II via MAP kinase signaling in cultured vascular smooth muscle cells. Anesthesiology 2002;96(1):148–154. [PubMed: 11753015]

Zhong L, Zhao W, Wu J, Li B, Zolotukhin S, Govindasamy L, Agbandje-McKenna M, Srivastava A. A Dual Role of EGFR Protein Tyrosine Kinase Signaling in Ubiquitination of AAV2 Capsids and Viral Second-strand DNA Synthesis. Mol Ther 2007;15(7):1323–1330. [PubMed: 17440440]

Zhong L, Zhou X, Li Y, Qing K, Xiao X, Samulski RJ, Srivastava A. Single-polarity recombinant adeno-associated virus 2 vector-mediated transgene expression in vitro and in vivo: mechanism of transduction. Mol Ther 2008b;16(2):290–295. [PubMed: 18087261]

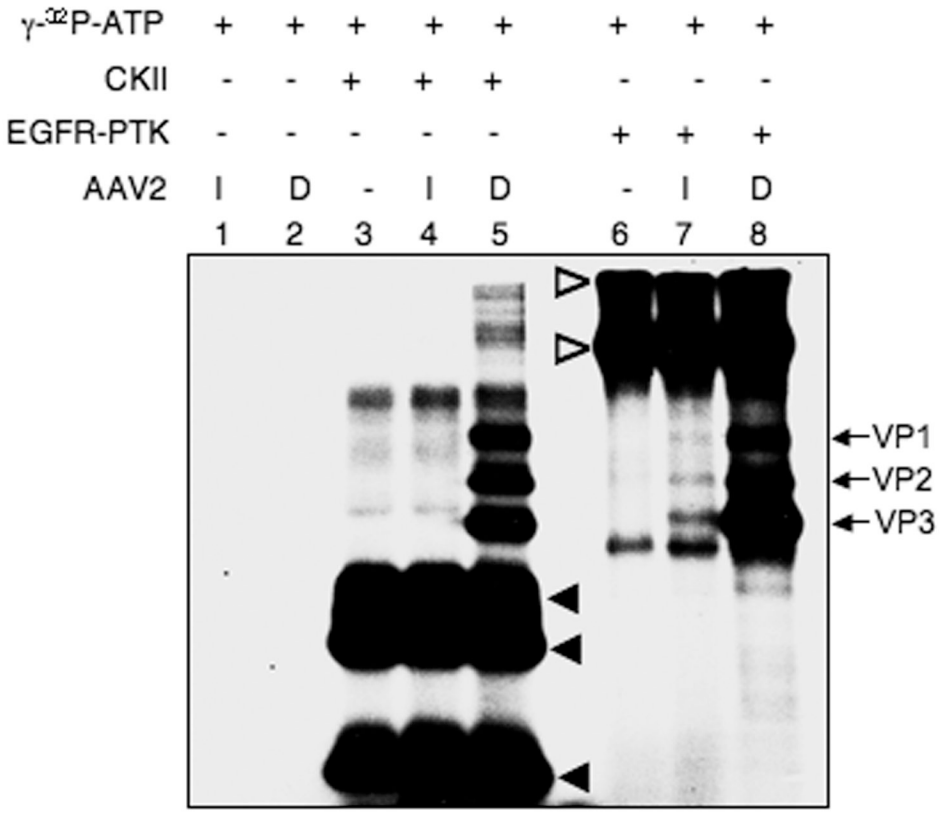


**Fig. 1.**

Autoradiographic image of SDS-polyacrylamide gel for *in vitro* phosphorylation of AAV2 capsids by CKII and EGFR-PTK. Approximately $4.8\times10^{10}$ particles of intact (I) and denatured (D) ssAAV2-adiponectin (K9) vectors were incubated in the absence of a protein kinase (lanes 1 and 2). CKII was incubated in the absence (lane 3) or presence of intact (I) (lane 4) or denatured (D) (lane 5) K9 vectors. Similarly, EGFR-PTK was incubated in the absence (lane 6) or presence of intact (I) (lane 7) or denatured (D) (lane 8) K9 vectors as described under Materials and Methods. The arrows indicate the phosphorylated forms of AAV2 capsid proteins, and the closed and open arrowheads denote the autophosphorylated CKII and EGFR PTK, respectively. These results are representative of two independent experiments.

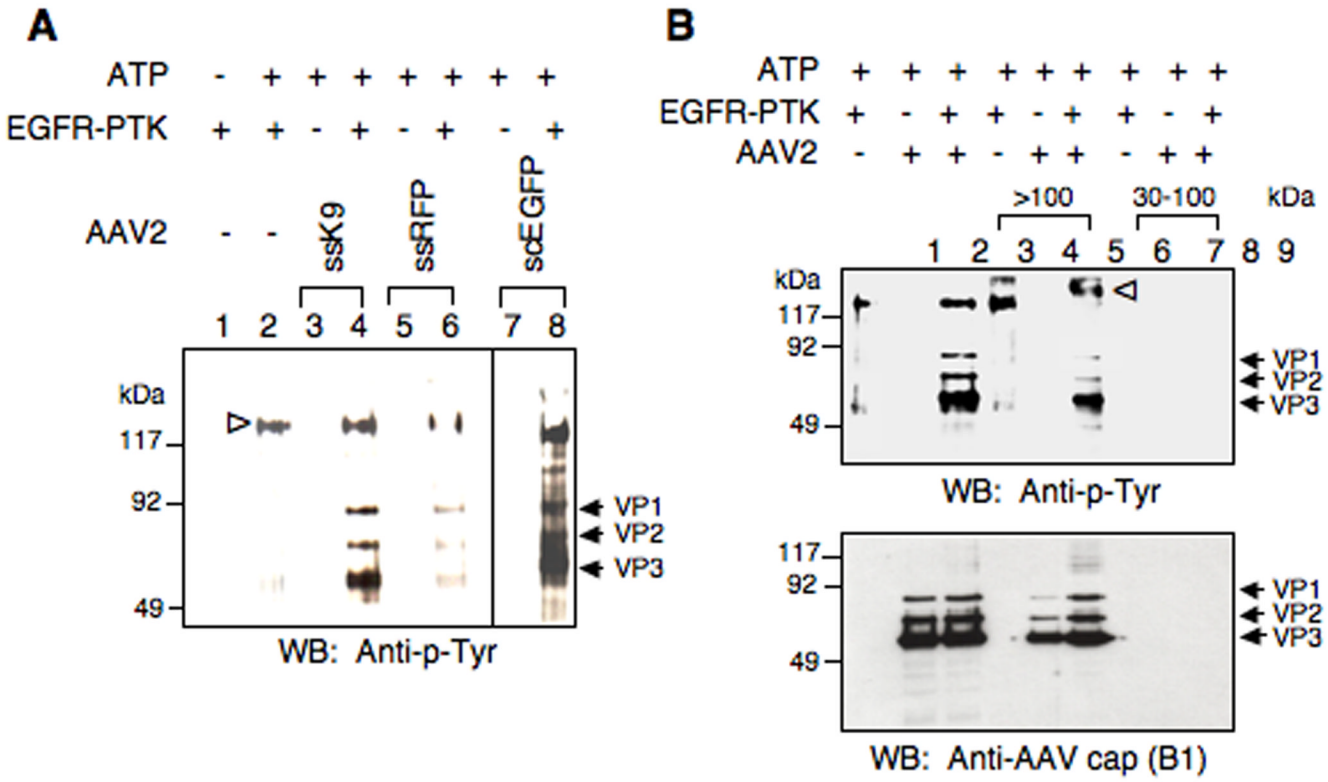


**Fig. 2.**

(A) Western blot analyses of *in vitro* phosphorylation of AAV2 capsids by EGFR-PTK from two different packaging systems. Approximately $3\times10^{10}$ particles of AAV2 vectors were incubated in the absence of EGFR-PTK (lanes 3, 5 and 7) and EGFR-PTK was mock-incubated (lane 1) or incubated in the absence (lane 2) or presence of AAV2 vectors (lane 4, 6 and 8) as described under Methods. The reaction samples were analyzed by Western blotting using anti-p-Tyr antibody for detection of phospho-tyrosine containing capsid proteins. The arrows indicate the phosphorylated forms of AAV2 capsid proteins, and the open arrowhead denotes the autophosphorylated EGFR-PTK. K9: AAV2-adiponectin (baculovirus-based AAV2 packaging system); RFP: ssAAV2-RFP (293 cells-based AAV2 packaging system); scEGFP: scAAV2-CBAp-EGFP (293 cells-based AAV2 packaging system). These results are representative of two independent experiments. (B) Western blot analyses of *in vitro* phosphorylation of AAV2 capsids by EGFR-PTK followed by separation of intact virions and free capsid proteins. Approximately $3\times10^{10}$ particles of AAV2 vectors were incubated in the absence of EGFR-PTK (lane 2) and EGFR-PTK was incubated in the absence (lane 1) or presence of AAV2 vectors (lane 3) followed by separation of > 100 kDa fraction (intact virions) (lanes 4, 5 and 6) and 30–100 kDa fraction (free capsid proteins) (lane 7, 8 and 9) using centrifugal filter devices [(Ultracel YM-100 (KD) and YM-30 (KD)] as described under Materials and Methods. The samples were analyzed by Western blotting using anti-p-Tyr antibody for detection of phospho-tyrosine containing capsid proteins (upper panel) and anti-AAV2 cap (B1) antibody for detection of total capsid proteins (lower panel). The arrows indicate the phosphorylated and total AAV2 capsid proteins, and the open arrowhead denotes the autophosphorylated EGFR-PTK.

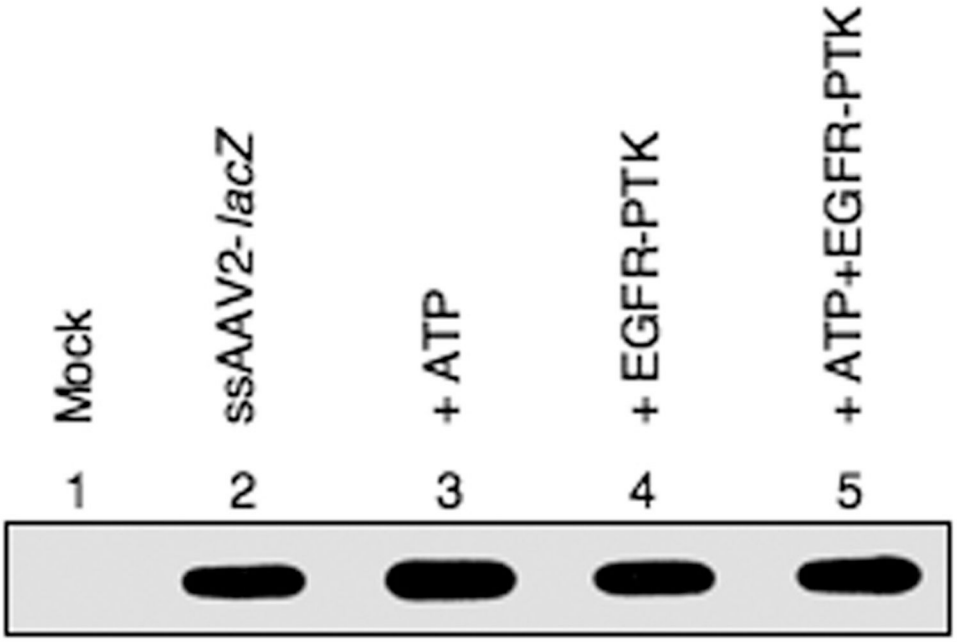


**Fig. 3.**

DNA slot blot analysis for AAV2 entry into HeLa cells after *in vitro* phosphorylation of AAV2 capsids by EGFR-PTK. HeLa cells were mock-infected (lane 1) or infected with AAV2-*lacZ* vectors, which were either mock-incubated (lane 2) or pre-incubated with ATP (lane 3), EGFR-TPK (lane 4) or both (lane 5). Following digestion with trypsin to degrade adsorbed and unadsorbed vectors, low-$M_r$ DNA samples were isolated 2 hrs post-infection and analyzed on by slot blot hybridization using a $^{32}$P-labeled *lacZ* DNA probe.

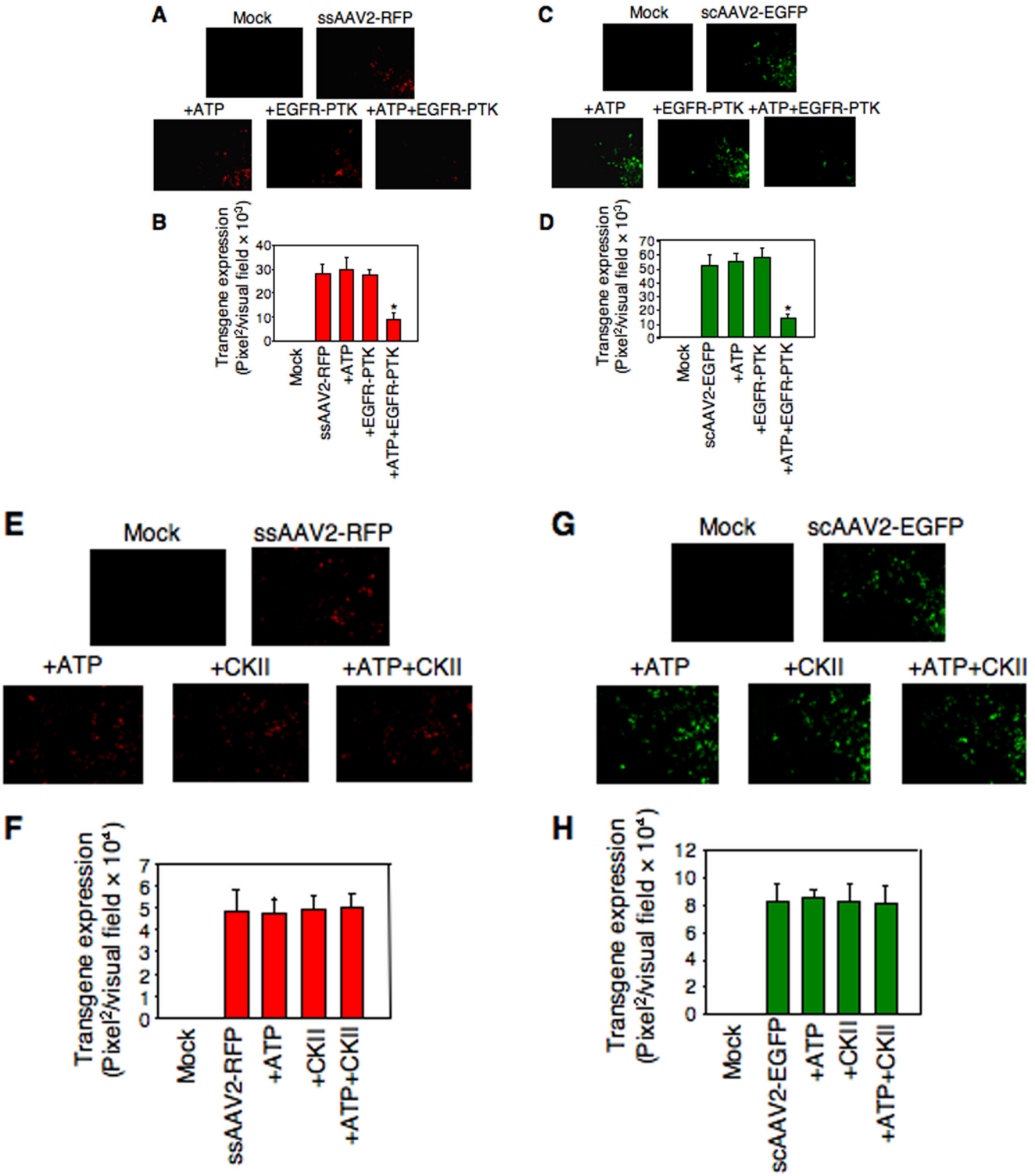


**Fig. 4.**

(A) Comparative analyses of AAV2-mediated transduction efficiency in HeLa cells after *in vitro* phosphorylation of AAV2 capsids by EGFR-PTK. HeLa cells were infected by ssAAV2-RFP vectors, which were pre-incubated with ATP, EGFR-TPK, or both. Transgene expression

was detected by fluorescence microscopy 48 hrs post-infection. Original magnification 100×. (B) Quantitative analyses of AAV2 transduction efficiency in HeLa cells. Images from five visual fields were analyzed quantitatively by ImageJ analysis software. Transgene expression was assessed as total area of red fluorescence (pixel$^2$) per visual field (mean ± SD). Analysis of variance (ANOVA) was used to compare test results with the control and they were determined to be statistically significant. *P < 0.05 *vs*. ssAAV2-RFP. (C) Infection of HeLa cells with scAAV2-EGFP vectors pre-incubated with ATP, EGFR-TPK, or both. Transgene expression was detected by fluorescence microscopy at 48 hrs post-infection. Original magnification 100×. (D) Quantitative analyses of AAV2 transduction efficiency was assessed as described above, and were determined to be statistically significant. *P < 0.05 vs. scAAV2-EGFP. (E) Comparative analyses of AAV2-mediated transduction efficiency in HeLa cells after *in vitro* phosphorylation of AAV2 capsids by CKII. HeLa cells were infected by ssAAV2-RFP vectors, which were pre-incubated with ATP, CKII, or both. Transgene expression was detected by fluorescence microscopy 48 hrs post-infection. Original magnification 100×. (F) Quantitative analyses of AAV2 transduction efficiency was assessed as described above. (G) Infection of HeLa cells with scAAV2-EGFP vectors pre-incubated with ATP, CKII, or both. Transgene expression was detected by fluorescence microscopy 48 hrs post-infection. Original magnification 100×. (H) Quantitative analyses of AAV2 transduction efficiency was assessed as described above.

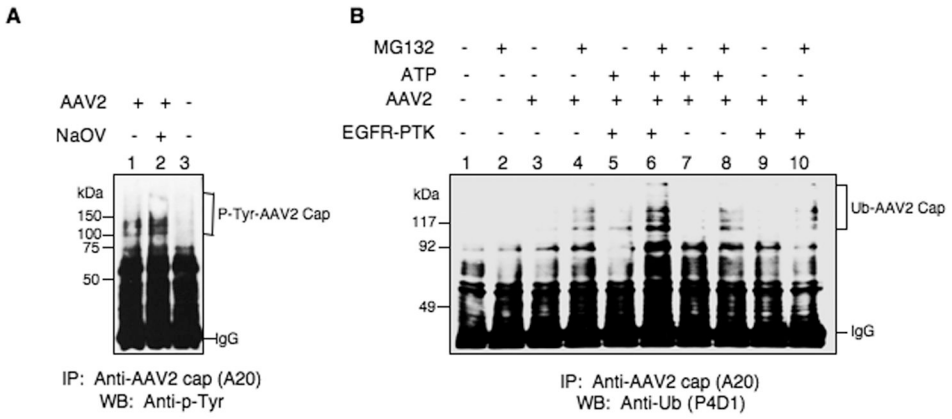


**Fig. 5.**

(A) Detection of intracellular tyrosine-phosphorylation of intact AAV2 vectors. Whole cell lysates (WCLs) prepared from HeLa cells untreated (lanes 1 and 3) or treated with NaOV (lane 2) following infection with K9 vectors (lanes 1 and 2) or mock-infection (lane 3), were immuno-precipitated with anti-AAV2 capsid antibody A20 followed by Western blot analyses with anti-p-Tyr antibody. (B) Detection of intracellular ubiquitin-conjugation of intact AAV2 vectors after *in vitro* phosphorylation of viral capsids by EGFR-PTK. Western blot analyses of ubiquitinated AAV2 capsid proteins in HeLa cells following transduction with ssAAV2-K9 vectors after *in vitro* phosphorylation of viral capsids by EGFR-PTK. Whole cell lysates (WCLs) prepared from HeLa cells untreated or treated with MG132 following mock-infected (lanes 1 and 2), or infected with K9 vectors, which were mock-incubated (lanes 3 and 4), or incubated with ATP (lanes 7 and lane 8), EGFR-PTK (lanes 9 and 10) or both (lanes 5 and 6), were immuno-precipitated with anti-AAV2 capsid antibody A20 followed by Western blot analyses with anti-Ub monoclonal antibody P4D1. This result is representative of two independent experiments.

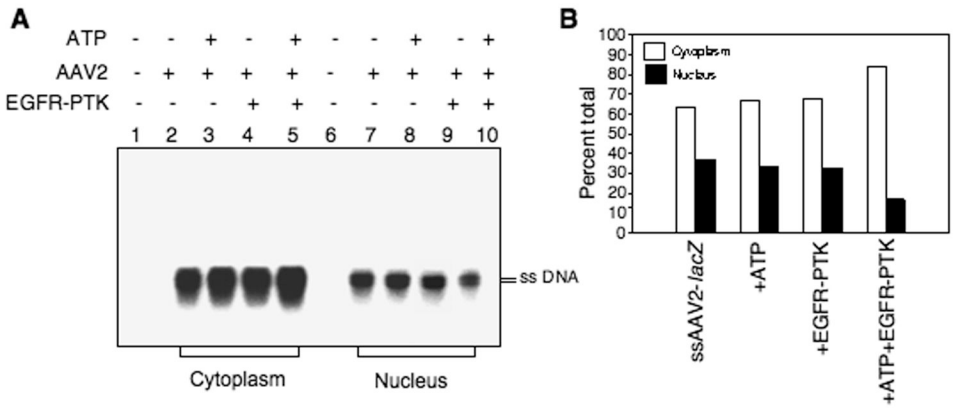


**Fig. 6.**

Detection of intracellular trafficking of AAV2 vectors to the nucleus after *in vitro* phosphorylation of viral capsids by EGFR-PTK. (A) Southern blot analyses of cytoplasmic and nuclear distribution of AAV2 genomes in HeLa cells after *in vitro* phosphorylation of AAV2 capsids by EGFR-PTK. HeLa cells were mock-infected (lanes 1 and 6) or infected by AAV2-*lacZ* vectors, which were mock-incubated (lanes 2 and 7) or pre-incubated with ATP (lanes 3 and 8), EGFR-TPK (lanes 4 and 9) or both (lanes 5 and 10). Nuclear and cytoplasmic fractions were prepared 18 hrs post-infection, low-Mr DNA samples were isolated and electrophoresed on 1% agarose gels followed analyzed by Southern blot hybridization using a $^{32}$P-labeled *lacZ* DNA probe. (B) Densitometric scanning of autoradiographs for the quantitation of relative amounts of viral genomes. These results are representative of two independent experiments.